

# Heavy-ion induced two-neutron transfer reactions and the role of pairing

M. Cavallaro<sup>1</sup>, C. Agodi<sup>1</sup>, F. Cappuzzello<sup>1,2</sup>, D. Carbone<sup>1</sup>, J.L. Ferreira<sup>3</sup>, A. Foti<sup>2,4</sup>, V. N. Garcia<sup>3</sup>, A. Gargano<sup>5</sup>, S. M. Lenzi<sup>6</sup>, R. Linares<sup>3</sup>, J. Lubian<sup>3</sup>, G. Santagati<sup>1</sup>

<sup>1</sup>Istituto Nazionale di Fisica Nucleare, Laboratori Nazionali del Sud, Catania, Italy.

<sup>2</sup>Dipartimento di Fisica e Astronomia, Università di Catania, Catania, Italy.

<sup>3</sup>Instituto de Física, Universidade Federal Fluminense, Niteroi, RJ, Brazil

<sup>4</sup>INFN Sezione di Catania, Catania, Italy

<sup>5</sup>INFN Sezione di Napoli, Napoli, Italy

<sup>6</sup>INFN Sezione di Padova, Padova, Italy

manuela.cavallaro@Ins.infn.it

## Abstract

Heavy-ion induced two-neutron transfer reactions ( $^{18}\text{O}, ^{16}\text{O}$ ) at 84 MeV were studied on several targets up to high excitation energy of the residual nucleus thanks to the use of the MAGNEX magnetic spectrometer to detect the ejectiles. The obtained results indicate of the important role played by the nuclear pairing.

*Key words:* heavy ions; transfer reactions; neutron transfer; magnetic spectrometers; VAN DE GRAAFF accelerators; energy spectra.

## Heacciones de transferencia de dos neutrones inducidas por iones pesados y el papel del apareamiento

### Resumen

Se estudiaron reacciones de transferencia de dos neutrones inducidas por iones pesados ( $^{18}\text{O}, ^{16}\text{O}$ ) a 84 MeV en varios blancos hasta una alta energía de excitación del núcleo residual gracias al uso del espectrómetro magnético MAGNEX para detectar los residuos eyectados. Los resultados obtenidos indican el importante papel desempeñado por el apareamiento nuclear.

*Palabras clave:* iones pesados; reacciones de transferencia; transferencia de neutrones; espectrómetros magnéticos; aceleradores VAN DE GRAAF; espectros de energía.

## Introduction

It is well known that the atomic nucleus is a complex many-body system. The knowledge of the internal degrees of freedom is crucial to understand nuclear structure features like single-particle and collective states, clustering, pairing correlations, and other properties [1]. This information can be extracted from elastic, inelastic, transfer, and other nuclear reactions. Transfer reactions have been extensively studied during the last decades because of their sensitivity to the nuclear structure of the interacting partners. In particular, two-nucleon transfer reactions have gained special attention because they can probe pairing correlations in nuclei [2], [3], [4], [5], [6], [7]. In addition, they are relevant to model more complex processes such as double charge exchange reactions, which are of interest for applications in neutrinoless double beta decay researches [8], [9].

In the last few years, a study of different systems was pursued at the Catania INFN-LNS laboratory (Italy) by the ( $^{18}\text{O}, ^{16}\text{O}$ ) two-neutron transfer reaction at 84 MeV

using the MAGNEX large acceptance magnetic spectrometer to detect the ejectiles. Thanks to its high resolution and large acceptance, high quality inclusive spectra have been obtained, even in a largely unexplored region above the two-neutron emission threshold in the residual nucleus.

New phenomena appeared, such as the dominance of the direct one-step transfer of the two neutrons and the presence of broad resonances at high excitation energy in the  $^{14}\text{C}$  and  $^{15}\text{C}$  spectra [2], [10]. These structures were recently identified as the first experimental signature of the Giant Pairing Vibration (GPV) [11], [12], [13] predicted long time ago [14].

## Materials and methods

### The experiments

The experiments were performed at the INFN-LNS laboratory in Catania. The beam of  $^{18}\text{O}^{6+}$ , accelerated at 84 MeV incident energy by the Tandem Van de Graaf,

impinged on different thin solid targets (namely  $^9\text{Be}$ ,  $^{11}\text{B}$ ,  $^{12}\text{C}$ ,  $^{13}\text{C}$ ,  $^{16}\text{O}$ ,  $^{28}\text{Si}$  and  $^{64}\text{Ni}$  targets) produced by evaporation at the LNS chemical laboratory. The beam-integrated charge was measured by a Faraday cup mounted 15 cm downstream of the target. So absolute cross-sections were extracted.

The ejectiles of  $^{16}\text{O}$  were momentum analysed by the MAGNEX spectrometer working in the full acceptance mode (solid angle  $\Omega \sim 50$  msr and momentum range  $\Delta p/p \sim 24\%$ ) [15], [16], [17]. In the different experimental runs, the optical axis of the spectrometer was centered at laboratory angles  $\theta_{\text{opt}} = 6^\circ, 12^\circ, 18^\circ, 24^\circ$ . In all the runs the ejectiles trajectory were accepted between  $-5.2^\circ$  and  $+6.3^\circ$  in the horizontal direction and  $\pm 7.0^\circ$  in the vertical, with respect to the optical axis. In such a way, an angular range between about  $3^\circ$  and  $30^\circ$  was measured in the laboratory frame with overlaps of about  $6^\circ$  between two contiguous sets of measurements.

### The energy spectra

Thanks to the spectrometer high resolution and large acceptance, high quality inclusive spectra were extracted, even in a largely unexplored region above the two-neutron separation energy in the residual nucleus [19], [20], [21], [21], [23], [24], [25].

Examples of the obtained excitation energy  $E^* = Q_0 - Q$  (where  $Q_0$  is the ground to ground state Q-value) spectra are shown in Fig. 1 for different targets and angular settings. For example, in Fig. 1 a) the  $^{14}\text{C}$  spectrum at  $9^\circ < \theta_{\text{lab}} < 12^\circ$  is represented. Several known  $^{14}\text{C}$  excited states are populated for which the spin and parity have been determined by previous (t,p) reactions [26]. It is known [27] that the dominant configuration of the ground state and the states at 7.01 and 10.74 MeV is a pair of two neutrons with  $L = 0, 2$  and  $4$  on a  $^{12}\text{C}$   $0^+$  core, respectively. It is very interesting to note that this spectrum is very similar to the ones excited by (t,p) reactions, indicating the strong selectivity of the ( $^{18}\text{O}$ ,  $^{16}\text{O}$ ) reaction. The energy spectrum for the  $^{13}\text{C}(^{18}\text{O}, ^{16}\text{O})^{15}\text{C}$  reaction in the angular range  $9.5^\circ < \theta_{\text{lab}} < 10.5^\circ$  is shown in Fig. 1b). The two bound states of  $^{15}\text{C}$  are recognized below the one-neutron separation energy ( $S_n = 1.218$  MeV), namely the ground and the state at 0.74 MeV. These are characterized by a well-known single-particle configuration with the valence neutron in the  $2s_{1/2}$  and  $1d_{5/2}$  shell over a  $^{14}\text{C}$   $0^+$  ground state core, respectively. Above  $S_n$ , narrow resonances at excitation energy of  $E^* = 3.10, 4.22, 4.66, 6.84, 7.35$  MeV are clearly identified. Such states are typically labeled as 2-particles-3-holes configurations and are strongly excited also by the (t,p) reaction reported in Ref. [28]. Above the two-neutron emission threshold ( $S_{2n} = 9.394$  MeV), two large unknown structures are strongly excited at  $E^* = 10.5$  and  $13.7$  MeV over a continuously distributed strength due to the three-body and four-body phase-spaces. A more detailed analysis of the two-neutron transfer on the  $^{15}\text{C}$  continuum is reported in Ref. [29].

Another interesting feature of the  $^{14}\text{C}$  and  $^{15}\text{C}$  spectra in Figure. 1 a) and b) is the appearance of two new structures above the two-neutron emission threshold at

$16.9 \pm 0.1$  MeV and  $13.7 \pm 0.1$  MeV, respectively. By a detailed analysis of these structures, reported in refs. [11], [12], [13], they were recently identified as the first experimental signature of the Giant Pairing Vibration (GPV) predicted long time ago [14].

In Figure. 1c) some results concerning the experiments on  $^{11}\text{B}$  target are shown. In ref. [20] a first evidence of pairing correlation was already discussed in presenting the transfer yields. Here we focus on the  $^{13}\text{B}$  energy spectra, where several peaks corresponding to transitions to known bound and resonant states and a broad structure between 10 and 14 MeV are observed. In particular, the states at  $E^* = 3.68, 4.13, 5.39, 6.16, 6.43$  and  $8.14$  MeV are the most populated. It is interesting to describe  $^{13}\text{B}$  low-lying states in the limit of a weak coupling among the  $3/2^-$  proton hole orbital and the  $^{14}\text{C}$  excited states. In this way, a direct link is established between  $^{13}\text{B}$  and  $^{14}\text{C}$  states at low excitation energy, which are characterized by the correlations of two neutrons in the sdshell. In comparing such homologous states, an interesting finding is the reduction of the energy of the  $^{13}\text{B}$  excited states of about 3 MeV compared to those of  $^{14}\text{C}$ . Since the ground state of both nuclei presents a  $N = 8$  magic number of neutrons, due to the p-shell closure, our finding indicates that the energy gap between p and sdshells is lowered from about 6 MeV in  $^{14}\text{C}$  to about 3 MeV in  $^{13}\text{B}$ . As a consequence the rapid evolution of the shell structure towards  $^{12}\text{Be}$  is confirmed, indicating that the  $N = 8$  shell closure is dissolving when neutron-rich nuclei are considered.

An example of  $^{66}\text{Ni}$  energy spectrum is shown in Figure. 1 d). In this case the spectrum features are sensibly different from the light nuclei ones. A large bump is observed probably due to the convolution of the several peaks populated in this region, due to particularly favorable kinematical matching conditions [23]. However, one should notice that for such heavy nuclei the incident energy corresponds to 1.7 times the Coulomb barrier. Thus the dynamical conditions could be rather different compared for example to the  $^{13}\text{C}$  target case, where the energy is 3.2 times the Coulomb barrier. Specific analysis based on semi-classical transport equations in heavy-ion collisions have been published in [30].

### The angular distribution

The absolute cross section angular distributions of the identified peaks were extracted in a quite wide range at forward angles, according to the procedure described in Ref. [31]. From their analysis it was demonstrated that the ( $^{18}\text{O}$ ,  $^{16}\text{O}$ ) two-neutron transfer reaction can be used for quantitative spectroscopic studies of pair configurations in nuclear states [2], [3], [24], [25], [23], [32]. Examples of angular distributions for the transitions to the  $^{14}\text{C}$  ground state and  $^{15}\text{C}$  low-lying excited states are shown in Figure 2 and 3.

From a theoretical point of view, the Coupled Reaction Channel (CRC) approach is necessary to interpret such data. In ref. [2] the experimental absolute cross section of the one- and two- neutron transfer reactions induced by an  $^{18}\text{O}$  beam on a  $^{12}\text{C}$  target was reproduced

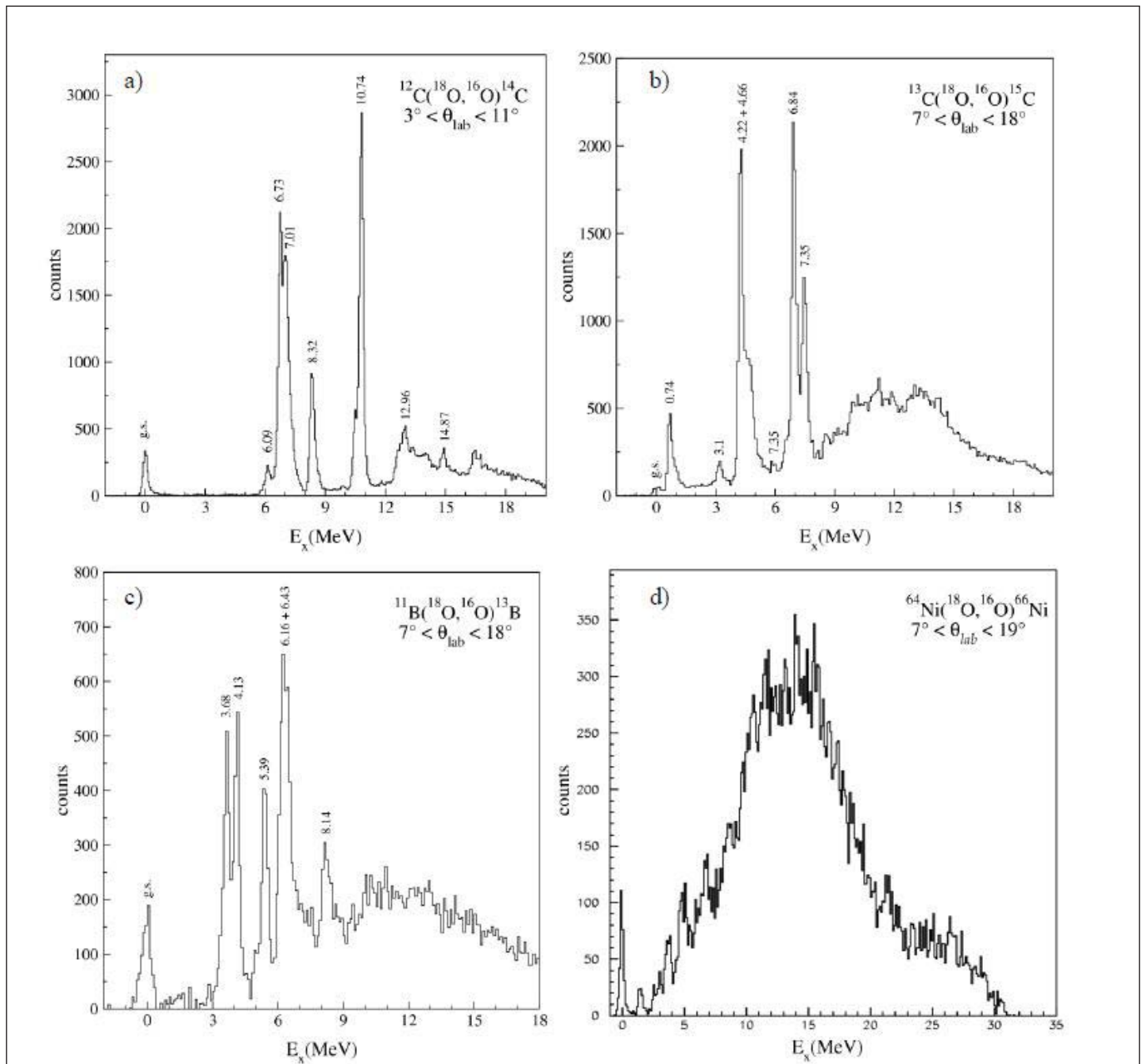


**Figure 1.** One-dimensional spectra of the reconstructed  $^{14}\text{C}$ ,  $^{15}\text{C}$ ,  $^{13}\text{B}$  and  $^{66}\text{Ni}$  excitation energy for the selected 160 ejectiles emitted in the  $(^{18}\text{O}, ^{16}\text{O})$  reaction at 84 MeV. The contribution due to the  $^{12}\text{C}$  impurities in the targets is subtracted in Fig.2 b), c) and d).

for the first time without the need of any scaling factor by means of Exact Finite Range (EFR) CRC calculations. Two approaches are shown here in this case: the extreme cluster model (where the two transferred neutrons are treated as a cluster system with the two neutrons coupled with relative spin  $S = 0$ ) and a sequential two-step approach. The relevance of cluster configurations was revealed in the ground state wave functions of the  $^{14}\text{C}$  nucleus, which was described within the extreme cluster approach, see Figure 2. On the other hand, the contribution of the sequential transfer mechanism appears small.

However, the strong approximation adopted in the extreme cluster approach makes it useful only in few cases, e.g. it does not describe well the higher excitation energy states [2]. In particular, in the case of the extreme cluster model with spectroscopic amplitudes set to 1,

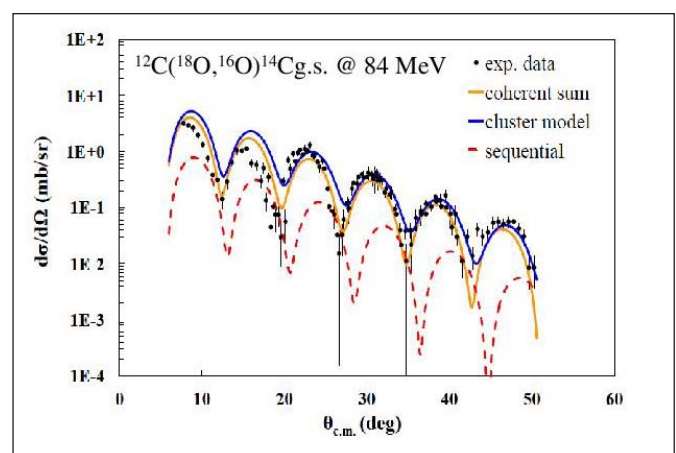


**Figure 2.** Comparison of the experimental angular distributions with theoretical calculations in extreme cluster model (blue), sequential (red) and coherent sum of the two processes (orange) for the  $^{12}\text{C}(^{18}\text{O}, ^{16}\text{O})^{14}\text{C.g.s.}$  reaction.

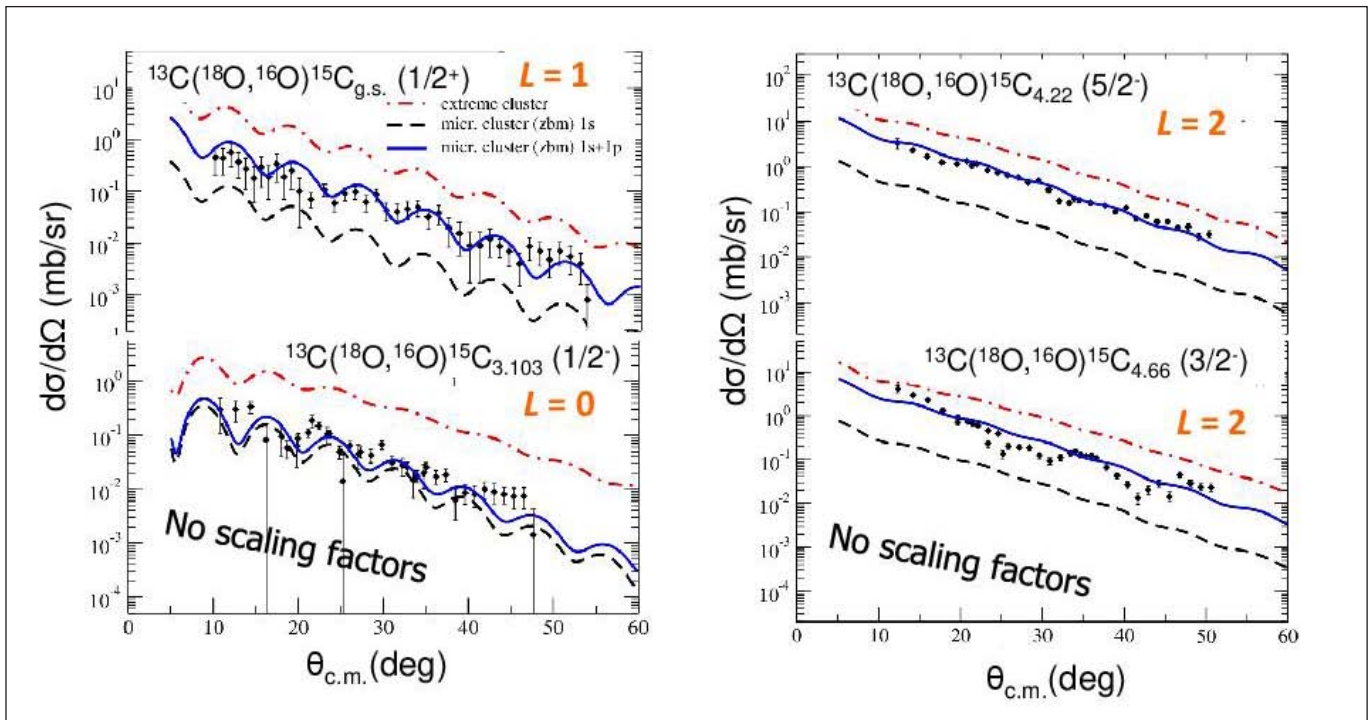


**Figure 3.** Comparison of the experimental angular distributions with theoretical calculations in extreme cluster model (red), microscopic cluster in the 1s state (black) and microscopic cluster in the 1s + 1p state (blue) for the  $^{13}\text{C}(^{18}\text{O}, ^{16}\text{O})^{15}\text{C}$  reaction populating different low-lying states of  $^{15}\text{C}$ .

often the calculated cross sections are larger than the experimental data. See for example the comparison with experimental data in the case of transitions to the  $^{15}\text{C}$  states shown in Figure 3. The main reason for this overestimation might lie in the approximation that the two neutrons are coupled to the total spin  $S = 0$  with 100% of probability. For this reason we developed in Ref. [32] a microscopic cluster model, where spectroscopic amplitudes from shell-model calculations. To achieve this objective, we made use of transformation brackets connecting the wave functions for two particles in an harmonic oscillator common potential ( $j$ - $j$  coupling) with the wave functions given in terms of the relative and centre of mass coordinates of the two particles ( $LS$  coupling). As a first step, we performed microscopic cluster calculations considering that the cluster relative motion state is represented exclusively by  $n = 1$  and  $l = 0$  quantum numbers, i.e. the cluster is in the 1s intrinsic state. The obtained cross sections (labelled 1s microscopic cluster) are much lower than data for all transitions. Thus, we included also the 1p ( $n = 1$  and  $l = 1$ ) cluster relative motion states (labelled 1s + 1p microscopic cluster). We see in Figure 3 that the 1s + 1p microscopic cluster calculations are in rather good agreement with the experimental angular distributions, without the need of any scaling factor.

The microscopic cluster model has allowed to well describe the experimental cross section, thus demonstrating the importance of a two-neutron correlation in the nuclear wave function in the two-neutron transfer mechanism. A dominance of the 1s and 1p waves in the two-neutron cluster internal wave function is found. This result show that the extra neutron in  $^{13}\text{C}$ , when compared

to  $^{12}\text{C}$ , does not destroy the neutron-neutron correlations in the wave functions.

## Acknowledges

This project has received funding from the European Research Council (ERC) under the European Union's Horizon 2020 research and innovation programme (grant agreement No 714625).

## References

- [1] SATCHLER GR. Direct nuclear reactions. Oxford: Oxford University Press, 1983.
- [2] CAVALLARO M, et. al. Quantitative analysis of two-neutron correlations in the  $^{12}\text{C}(^{18}\text{O}, ^{26}\text{O})^{14}\text{C}$  reaction. Phys. Rev. C 2013; 88(5): 054601.
- [3] CARBONE D, et. al. First application of the  $n$ - $^9\text{Be}$  optical potential to the study of the  $^{10}\text{Be}$  continuum via the  $(^{18}\text{O}, ^{17}\text{O})$  neutron-transfer reaction. Phys. Rev. C. 2014; 90: 064621
- [4] KAHANA S & BALTZ AJ. One nucleon and two nucleon transfer reactions with heavy ions. Adv. Nucl. Phys. 1977; 9: 1-22.
- [5] TAKEMASA T & YOSHIDA H. Analysis of two-nucleon transfer reactions by heavy ions on the basis of one- and two-step processes. Nucl. Phys. A. 1978, 304(1): 229.
- [6] LEMAIRE MC & LOW KS. Analysis of the  $^{74}\text{Ge}(^{18}\text{O}, ^{16}\text{O})^{76}\text{Ge}$  and  $^{76}\text{Ge}(^{16}\text{O}, ^{18}\text{O})^{74}\text{Ge}$  reactions in terms of exact finite-range coupled-channel born approximation. Phys. Rev. C. 1977; 16(2): 183.
- [7] POTEI G, et. al. Cooper pair transfer in nuclei. Rep. Prog. Phys. 2013; 76(10): 106301.
- [8] CAPPUZZELLO F, et. al. Heavy-ion double charge exchange reactions: a tool toward  $0\nu\beta\beta$  nuclear matrix elements. Eur. Phys. J. A. 2015; 51(11): 145.
- [9] CAPPUZZELLO F, et. al. The role of nuclear reactions in the problem of  $0\nu\beta\beta$  decay and the NUMEN project at INFN-LNSJ. Phys. Conf. Ser. 2015; 630(conference 1): 012018.



- [10] CAPPUZZELLO F, et. al. New structures in the continuum of  $^{15}\text{C}$  populated by two-neutron transfer. Phys. Lett. B. 2012; 711(5): 347-352.
- [11] CAPPUZZELLO F, et. al. Signatures of the giant pairing vibration in the  $^{14}\text{C}$  and  $^{15}\text{C}$  atomic nuclei. Nat. Commun. 2015; 6: 6743.
- [12] CARBONE D. Signals of the Giant Pairing Vibration in  $^{14}\text{C}$  and  $^{15}\text{C}$  nuclei populated by ( $^{18}\text{O},^{16}\text{O}$ ) two-neutron transfer reactions. Eur. Phys. J. Plus. 2015; 130:143.
- [13] PIEKAREWICZ J. Nuclear physics: two more or less. Nature physics. 2015; 11: 303-304.
- [14] BROGLIA RA & BES D. High-lying pairing resonances. Phys. Lett. B. 1977; 69: 129-133.
- [15] CAPPUZZELLO F, et. al. The MAGNEX spectrometer: results and perspectives. Eur. Phys. J. A. 2016; 52:157.
- [16] CAVALLARO M, et. al. Nuclear response to two-neutron transfer via the ( $^{18}\text{O},^{16}\text{O}$ ) reaction. Nucl. Instr. and Meth. A. 2011; 637: 77.
- [17] CAVALLARO M, et. al. The low-pressure focal plane detector of the MAGNEX spectrometer. Eur. Phys. J. A. 2012; 48: 59.
- [18] CAVALLARO M, et. al. States of  $^{14}\text{C}$  and  $^{15}\text{C}$  via the ( $^{18}\text{O},^{16}\text{O}$ ) two-neutron transfer reaction at 84 MeV. J. Phys.: Conf. Ser. 2012; 381(conference 1): 012094.
- [19] NICOLOSI D, et. al. Spectroscopy of  $^{13}\text{B}$  via the ( $^{18}\text{O},^{16}\text{O}$ ) two neutron transfer reaction. Acta Phys. Pol. B. 2013; 44(3): 657.
- [21] CARBONE D, et. al. Exploring the  $^{12}\text{C}(^{18}\text{O},^{16}\text{O})^{14}\text{C}$  two-neutron transfer reaction at energies far above the Coulomb barrier. J. Phys.: Conf. Ser. 2015; 590: 012030.
- [22] PAES B, et. al. Long-range versus short-range correlations in the two-neutron transfer reaction  $^{64}\text{Ni}(^{18}\text{O},^{16}\text{O})^{66}\text{Ni}$ . Phys Rev C. 2017; 96: 044612.
- [23] ERMAMATOV MJ, et. al. Comprehensive analysis of high-lying states in  $^{18}\text{O}$  populated with (t,p) and ( $^{18}\text{O},^{16}\text{O}$ ) reactions. Phys Rev C. 2017; 96(4): 044603.
- [24] ERMAMATOV MJ, et. al. Two-neutron transfer analysis of the  $^{16}\text{O}(^{18}\text{O},^{16}\text{O})^{18}\text{O}$  reaction. Phys Rev C. 2016; 94(2): 024610.
- [25] MORDECHAI S, et. al. Structure of  $^{14}\text{C}$  from  $^{12}\text{C}(t, p)$ . Nucl. Phys. A. 1978; 301(3): 463-476.
- [26] von OERTZEN W, et. al. Search for cluster structure of excited states in  $^{14}\text{C}$ . Eur. Phys. J. A. 2004; 21(2): 193-215.
- [27] TRUONG S & FORTUNE HT. 1p-2h and 2p-3h states in  $^{15}\text{C}$ . Phys. Rev. C. 1993; 28(3): 977.
- [28] CAPPUZZELLO F, et. al. New structures in the continuum of  $^{15}\text{C}$  populated by two-neutron transfer. Phys. Lett. B. 2012; 711(5): 347-352.
- [29] CAVALLARO M, et. al. The ( $^{18}\text{O},^{16}\text{O}$ ) reaction: a bridge from direct to dissipative dynamics. J. Phys.: Conf. Ser. 2014; 515(conference1): 012003.
- [30] CAVALLARO M, et. al. Transport efficiency in large acceptance spectrometers Nucl. Instr. and Meth. A. 2011; 637(1): 77-87.
- [31] CARBONE D, et. el. Microscopic cluster model for the description of new experimental results on the  $^{13}\text{C}(^{18}\text{O},^{16}\text{O})^{15}\text{C}$  two-neutron transfer at 84 MeV incident energy. Phys. Rev. C. 2017; 95(3): 034603.

**Recibido:** 13 de febrero de 2018

**Aceptado:** 29 de mayo de 2018